

ASSESSING THE VARIABILITY OF INTERNAL BRAIN STRUCTURES USING PCA ON SAMPLED SURFACE POINTS

Darwin Martínez^{1,2}, Isabelle Bloch¹ and José Tiberio Hernández¹

¹TELECOM ParisTech (ENST) - CNRS UMR 5141 LTCI, Paris, France

²Universidad Los Andes - Imagine Team, Bogotá, Colombia

Keywords: Anatomical variability, MRI images, Brain structures, Principal component analysis.

Abstract: In this paper we propose to analyze the variability of brain structures using principal component analysis (PCA). We rely on a data base of registered and segmented 3D MRI images of normal subjects. We propose to use as input of PCA sampled points on the surface of the considered objects, selected using uniformity criteria or based on mean and Gaussian curvatures. Results are shown on the lateral ventricles. The main variation tendencies are observed in the orthogonal eigenvector space. Dimensionality reduction can be achieved and the variability of each landmark point is accurately described using the first three components.

1 INTRODUCTION

Assessing the variability of natural objects has been the purpose of many works in different domains. Concerning human beings, the analysis of the variability of morphological or functional features permits a better description of the human body and its various components, a categorization of populations, and a study of differences between normal and pathological cases. The variability can be assessed from several sources, such as morphometric measurements or medical imaging. Conversely, in medical imaging, variability has also been used to guide segmentation and recognition applications in several works, for instance based on shape and appearance models (Hill et al., 1996; Cootes et al., 2001; Larsen and Hilger, 2003).

In this paper, we address the question of shape variability of normal internal brain structures, observed in 3D magnetic resonance imaging (MRI). The proposed framework relies on a surface-based representation of different samples of a given structure, leading to a matrix of landmark points, which is further analyzed using principal component analysis (PCA). This approach departs from similar works, where PCA is typically applied to distance maps characterizing the shapes (see e.g. (Pohl et al., 2004), among others). As an example, results are illustrated on the left ventricle, which presents an important inter-subject variability.

This paper is organized as follows. In Section 2 we summarize some related works about the variability measurements in human body and in other contexts. In Section 3 we address the representation issues. Two surface sampling methods are proposed, one relying on a regular subdivision of space, and one based on maximum curvature points. In Section 4 the estimation of the variability in a population using PCA is described. In Section 5 results on the left ventricles are provided and analyzed.

2 RELATED WORKS

Studying the variability of a structure from a set of instances of this structure allows us to characterize the diversity in this set. This estimation can be made using different techniques based on the analysis of some features of the structure to be analyzed.

In this paper we focus on human anatomical structures. However, inspiration can also be found in other domains of application.

2.1 Variability in Human Body

Many works aim at measuring the differences in the human body, usually focusing on specific organs. The objective can be to describe the normal anatomy along with its potential variations within a population, or to

assess the presence of some abnormality indicating some diseases.

In this section, we mention a few examples of works in this domain, with the aim of illustrating the variety of addressed problems. This list is of course far from being exhaustive.

In (Suinesiaputra et al., 2004) the authors model the myocardial contractility using independence component analysis (ICA) in order to identify the dysfunctional myocardium. The authors present a model of the two contours at distinct times (systole and diastole) to create a set of points in the middle of the contours in order to perform the measurements with ICA.

In (Lötjönen et al., 2004) the authors model the atria, ventricles and epicardium of the heart in a 3D shape, as a combination of short and long axis cardiac MR images. For this task the authors use a correspondence voxel by voxel and then construct a set of landmarks from the surface of the objects which are used as input to PCA and ICA algorithms in order to compute the shape variation.

In (Taron et al., 2007) the authors model the left ventricle as a thin plate spline. An additional estimation of registration uncertainties is included in the model before applying ICA to capture the variations.

In the work of (Berar, 2007) PCA is used to perform a statistical reconstruction of skull and face. Using PCA in combination with a feature space representation then produces a skull facial partial reconstruction.

In (Nain et al., 2007), the authors present a new strategy for multiscale shape representation and segmentation of internal brain structures, in particular caudate nucleus and hippocampus. The shape representation is based on conformal mapping and spherical wavelets adapted to a given population. Shape variations are determined using a spectral partitioning of coefficients. The experimental results show the power of this approach for capturing shape details and integrating the model in a segmentation framework.

In a different domain, in (Bai et al., 2007) the authors present ICA as a feature to find a similarity metric between different sets of fMRI, and the independent components are then used to describe the highly activated regions. In this way, the similarity between sets is evaluated as the value of the maximum size of overlap between regions corresponding to activation maps.

All these works show how different types of features are studied in order to keep the most representative data set, which is enough to evaluate the differences between elements. The selection of the representative set is an important step for posterior assess-

ment.

2.2 Variability in other Image Applications

Let us now briefly mention a few other examples, in other application domains.

In (Ekenel and Sankur, 2004) the authors focus on the problem of feature selection for face recognition and they propose a method to examine the subsets of ICA and PCA features in order to increase recognition performance. For PCA they take the eigenvalues, while for ICA they made some tests in order to select the most descriptive/difference features.

In (Yang and Ding, 2002) the authors use a combination of PCA and a symmetry plane (mirror) to search the faces in a series of images. They divide the space based on the mirror of the faces and apply PCA to characterize the important elements in the face and define the variations modes of each side.

In (Rogez and Orrite, 2005) the authors use ICA and PCA in order to compute the variations of the human figure, and they model the human body as the contour of the silhouette. Then they construct a mean shape and use it as basis to find the differences of the silhouette.

These studies present the analysis of variability using the combination of PCA and ICA to identify the sources of variation from global context using PCA and local context using ICA. The studies show clearly the difficulty to select the correct number of variation modes in ICA.

In summary, there are two main aspects to consider:

1. Shape representation: a concise representation scheme has to be determined that will allow a comparison between different individuals based on the represented shape.
2. Analysis technique: it should make it possible to characterize and localize the shape variability in the studied family, in such a way that a new individual can be characterized based on that analysis.

3 SHAPE REPRESENTATION

In our experiments, we use the MRI images of the IBSR database¹, which contains a set of images from

¹Internet Brain Segmentation Repository. The MR brain data sets and their manual segmentations were provided by the Center for Morphometric Analysis at Massachusetts General Hospital and are available at <http://www.cma.mgh.harvard.edu/ibsr/>

18 normal subjects, and for which a segmentation of the main anatomical structures is available.

From these segmented images, we select one structure of interest that will be subject to variability analysis. For illustration purposes, we consider the left lateral ventricle as a typical example (see Figure 1).

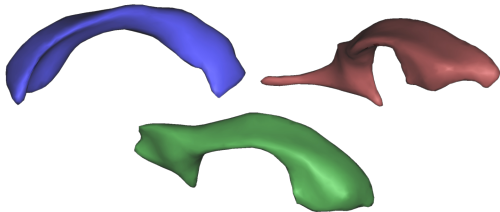


Figure 1: Left lateral ventricles from three different subjects of the IBSR database, illustrating the variability of the shape of this structure.

The first step in our approach consists in constructing the set of elements on which PCA will be applied. These elements are points of the object under study (i.e. one particular anatomical structure), observed on several subjects. They should be a good representation of the shape of the object. In this section, we describe the chosen representations.

Usually, a representation is chosen according to one or several criteria, such as expressiveness of the representation (information it provides, precision of the description), possibility of reconstructing the object, and complexity of the representation (costs it induces on storage space and computation time).

For our application, we need a representation of 3D objects that has a reasonable size, while preserving the information quality. This issue is particularly important in medical imaging. The MRI images used in this work have a spatial resolution of about 1mm^3 and contain about $8 \cdot 10^6$ points. Even if a particular anatomical structure only occupies a restricted part of this volume, the amount of data to be processed increases rapidly. This is amplified here by the fact that several images of different subjects are used in each computation step. This advocates for a sampling of the objects in order to derive the representation.

Since we are dealing with simply connected objects, which are adequately represented by their surface, we choose a surface sampling approach. The gain in the representation, with respect to volumetric sampling, depends on the shape of the object (high for a spherical object, low for an almost linear one), but is in all cases appreciable.

In this paper, we propose to use two types of sampling. The first one relies on a systematic and regular decomposition of the space, while the second one is

shape-dependent and relies on high curvature points.

We denote by S_i the surface of a given structure in image i ($i = 1..M$), and by x_i^j the j th sampled point on S_i ($j = 1..N$). The matrix $X = ((x_i^j))$ will be the input of PCA (see Section 4).

3.1 Description based on Regular Grid

This approach relies on a simple regular subdivision of the bounding box of S_1 . The landmark points x_i^j are then defined as the intersections between the planes defining the subdivision and S_1 . This is illustrated in Figure 2.

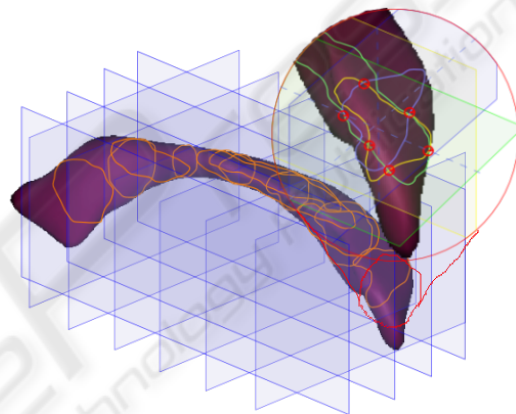


Figure 2: Regular grid subdivision of the bounding box of a structure and induced surface sampling.

These points are then projected on the other examples of the structures S_i , for $i = 2..M$, using the ICP method (Besl and McKay, 1992). This guarantees a good correspondence between x_i^j and $x_{i'}^j$ for all j and all examples S_i and $S_{i'}$. This correspondence is required in order to be sure that the variability analysis is based on similar features.

3.2 Curvature-based Description

The second approach we propose is to build the description from remarkable points on the surface, derived from curvature information. This approach is similar to the one developed in (Moreno et al., 2007; Moreno et al., 2008) for constrained registration of lung images. It is motivated by the fact that points with high curvature are particularly relevant for describing a shape and distinguishing between different shapes. We argue that they are also relevant for descriptions aiming at variability analysis.

The proposed procedure is as follows. The Gaussian and mean curvatures (defined as the product and the average of the principal curvatures, respectively)

are computed at all points of S_i . This computation is based on a finite difference approximation of the derivatives.

Then two ordered lists of points are built, with decreasing absolute value of Gaussian (respectively mean) curvature.

Landmark points are selected starting from the highest curvature points, by picking alternatively from the two ordered lists. An additional constraint is added in order to have an almost uniform distribution on the surface: a point is selected only if its distance to already selected points exceeds some pre-set threshold. The distance is computed conditionally to the surface (i.e. geodesic distance), using a propagation method, like the classical chamfer algorithm (Borgefors, 1986), adapted to the geodesic case (the masks defining the local distances and used for propagation are restricted to the surface points at each position during the propagation).

In order to deal with potentially flat areas, zero curvature points are considered as well, so as to guarantee the uniformity constraint. The results on one example are displayed in Figure 3.

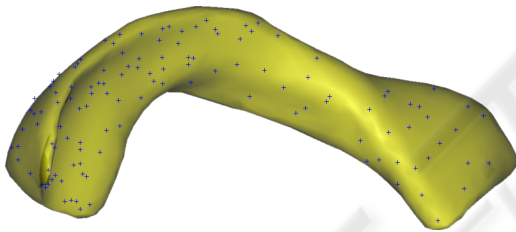


Figure 3: Distribution of points based on curvature calculus.

Finally, the selected points $x_1^j, j = 1..N$ are used to find the corresponding points of the other examples $S_i, i \neq 1$, again using the ICP method. It should be noted that the projected points do not necessarily correspond to the highest curvature points of S_i . However, they are close to those points (see Figure 4), and provide an appropriate representation of the shape. The fact that similar landmark points are used in all objects is important for the next steps, and this is guaranteed by the proposed approach.

The obtained landmarks provide an homogeneous description of the shape, thanks to the distance constraint, and rely on significant points, thanks to the curvature constraint. The correspondence between these landmarks in all shape examples provides the necessary information for variability analysis.

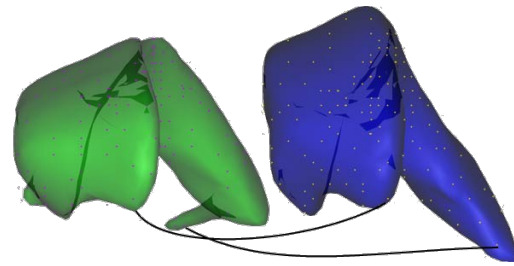


Figure 4: Landmark points computed on S_1 and their corresponding points obtained using ICP on another example S_i .

4 VARIABILITY MEASURES BASED ON PCA

The choice of principal component analysis (PCA) as a technique to model the variability among elements of the same type is driven by its powerful feature of proposing an order using the variance of the representative data of the examples of the analyzed set.

PCA is an orthogonal linear transformation between one data coordinate system to a new coordinate system such that the new system takes advantage of the variance associated to each axis. The components are ordered according to the variance value and the projections of the data on the first components express the largest variations.

The landmarks x_i^j , for $i = 1..M$ and $j = 1..N$, are organized in a matrix X where each row X_i is built from the coordinates of the landmarks computed on S_i (i.e. each row has $3N$ components).

In order to minimize the variation induced by the differences in the position (as illustrated in Figure 5) each shape is centered: the center of gravity of each set $(x_i^j), j = 1..N$ is computed and subtracted from x_i^j . It follows that all shapes are registered, with their new center of gravity equal to the origin of the space. Moreover, this also achieves the zero mean distribution constraint imposed when applying PCA. For sake of simplicity, we still denote by X the matrix obtained after this registration step. Figure 6 illustrates the set of centered structures.

The next steps consist of a classical application of PCA: the covariance matrix of the centered data $C = XX^T$ is computed. Then its eigenvectors V and eigenvalues D are computed. The eigenvalues are sorted in decreasing order. We denote by D_o the vector of ordered eigenvalues and V_o the corresponding matrix of eigenvectors. The columns of V_o are then the principal components.

By analyzing the variance of each component and its contribution to the global variation we can select how many components should be taken into account

to represent the variability. Usually, only a few components are sufficient, thus leading to a reduced dimensionality.

Then we compute the projection of the centered data on the new orthogonal space for each of the selected components. We denote by $P_k = V_o^k X$ the k th projection where V_o^k is the k th component of V_o . Finally, we reconstruct the objects in the original space by computing $\tilde{X}_k = P_k^{-1} X$ for each of the selected components. By adding again the mean value that was subtracted during the registration step, we obtain a comparable set of data. For instance, if the first component is selected, then P_1 is the projection of the data onto the first principal component and \tilde{X}_1 , which is an $M \times 3N$ matrix, contains the projection of the first principal component for each of the M samples.

In our experiments with 3D data, we obtain, for each landmark and for each component of variation mapped onto the original space, the direction and magnitude of data variation in that direction.

5 EXPERIMENTS AND RESULTS

In this section, we illustrate the proposed approach on the analysis of the left lateral ventricle (as illustrated in Figure 1). We used the manual segmentations available for the 18 examples of the IBSR database. The images in the data base are globally registered and have been “positionally normalized” into the Talairach orientation (rotation only). The left lateral ventricles of the data base are shown in Figure 5. As mentioned in Section 4, a further registration based on a translation matching all centers of gravity is also applied. The centered shapes are displayed in Figure 6. This registration guarantees position normalization and avoids interpreting the difference in absolute position as a variability factor.

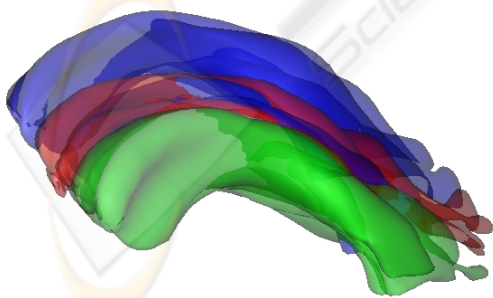


Figure 5: The 18 left lateral ventricles of the IBSR database.

The general scheme of the processing is illustrated in Figure 7. From the segmented objects, sampled points are computed using the two methods described in Section 3. Then PCA is applied on the resulting

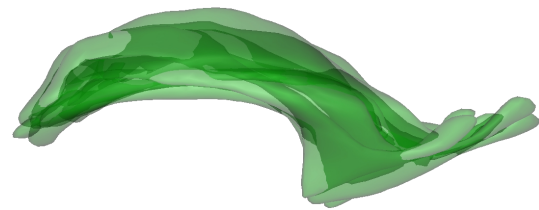


Figure 6: Set of centered structures.

matrices, as described in Section 4. The results are analyzed based on the reconstruction using the main components and the variance.

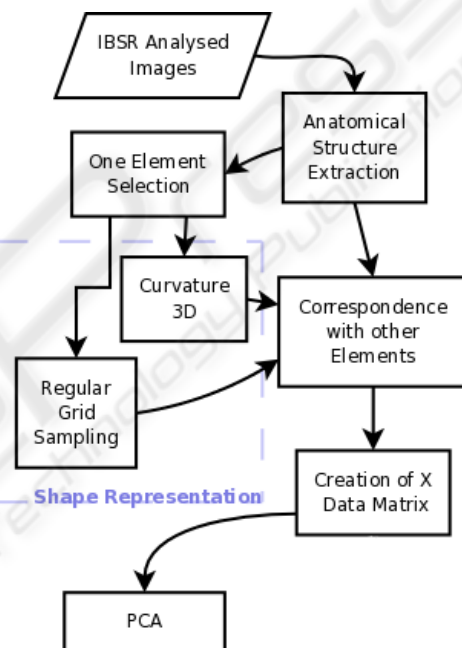


Figure 7: Experiment flowchart.

The results depend on the following parameters:

- density of samples;
- choice of the distribution (regular, based on curvature);
- the number of main components in the reconstruction.

In order to test the shape representation approaches presented in section 3, both set of results are presented (curvature and regular grid based models) below. The figures 8 to 12 have been obtained with a selection of landmark points based on curvature information. On the first example S_1 , 136 points are selected according to the highest curvature and uniformity criteria, and the corresponding points are then computed on all other 17 examples. This results in a 18×408 matrix. The initial surfaces contain

about 2400 points in average, which makes a density of 0.06.

Applying the proposed approach to the left lateral ventricle leads to the following results:

- The principal component analysis made it possible to explain 75.67% of the variation of the left lateral ventricle (Figure 8) with only three components.

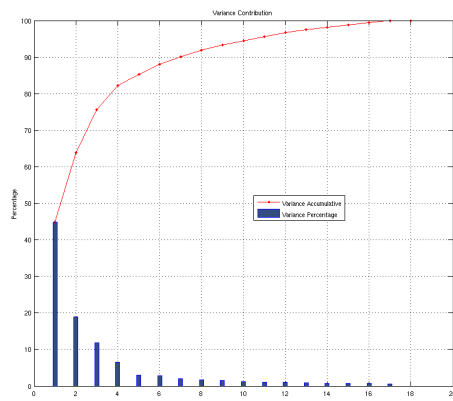


Figure 8: Variance of each of the principal components and its contribution to the total variation.

- The first principal component represents 44.9% of the variance in the set of shapes. Thus, with this only component we can express almost the half of the variance of the whole set. Figure 9 represents the first mode of variation projected in the original data space. Each point indicates the mean of the landmark, while the line segments indicate the direction and magnitude. These segments do not exhibit strong structures, thus expressing each local variation of the shapes.

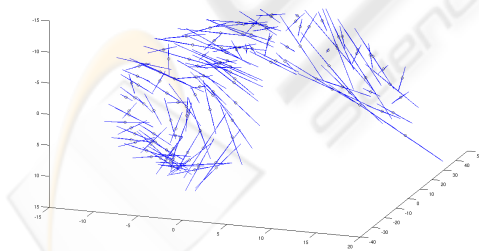


Figure 9: First Component.

- The second principal component represents 18.94% of the variance. It is illustrated in Figure 10. It shows a kind of torsion between the different shapes (the segments have a quite consistent organization).
- The third principal component represents 11.83% of the variance, and is shown in Figure 11. The

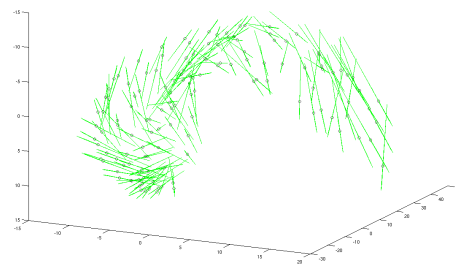


Figure 10: Second Component.

orientation of the segments on the right part of the figure can be interpreted as a variance of the global curvature of the shape.

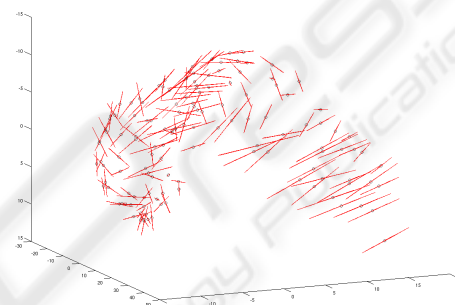


Figure 11: Third Component.

Figure 12 presents the results of the three first components projected in the original space. It illustrates the variation of all landmarks in the data set and the representation and contribution to the variance of each landmark to the total variation. It also shows that all landmarks have a similar contribution to the variability and that it is difficult to assign the variation to a particular subset of landmarks. This result was expected because PCA estimates the differences of a set of samples (anatomical structures in this case) against the mean values of the samples.

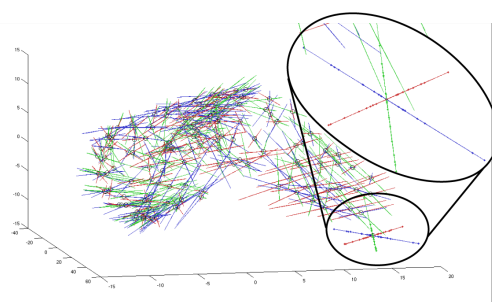


Figure 12: Three first components.

The zoomed area in Figure 12 shows the influence of each component (blue: first component, green: second component, red: third component). The inter-

section of the three components corresponds to the mean value of the landmark, and each little point on the segment line represents the value of one projected sample. This illustrates the range of variation of the landmark and the set of points on each of the segment lines shows an interesting distribution. We think that it is an important characteristic that has to be evaluated in the future because it can give us more specific information about the variability in a population.

The results illustrated in the figures 13 and 14 have been obtained with a selection of landmark points based on the regular grid division. For this example (S_2) 216 points are selected according of the division by 10 of each side of the bounding box. The point density over the surface is about 0.09% , which is similar to the density we had in the curvature-based point distribution. The corresponding points are computed on all the other 17 examples, leading to a 18×648 matrix to compute PCA.

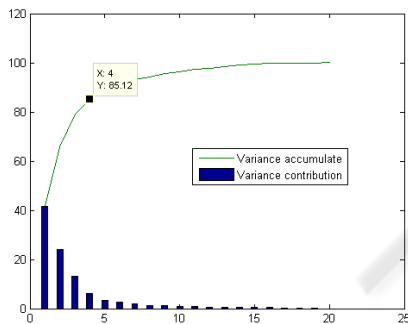


Figure 13: Variance contribution using a point distribution based on a regular grid.

The type of distribution (regular grid vs. curvature based) does not affect representatively the variance contribution of the components, as shown in Figure 13. This figure is similar to Figure 8.

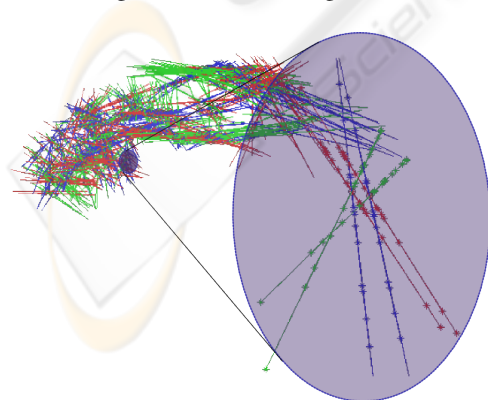


Figure 14: Three first components on regular grid. Zoom in two nearest points.

Although, regular grid representation is attractive

due to its simplicity and regularity, the model presents some disadvantages: first, it can miss some important points (hidden points) for the shape representation and second, there is oversampling of points in some shape sectors due to element form as is presented in Figure 14. The hidden points and oversampling are risky for shape representation, and that is why it is recommendable to use the curvature based model and the geodesic distance on the surface, in spite of its simplicity and computational performance (1 / 10, regular grid / curvature).

6 CONCLUSIONS

In this paper, we have proposed a method for the study of shape variability of anatomical structures in the human brain using information extracted from magnetic resonance images. The main features of the method are:

- representation of the surface of the structures, for which two methods have been proposed for landmark selection, as well as a correspondence between points of different examples;
- construction of a data set with zero mean in each sample in order to reduce the influence of position variation between the structures;
- use of PCA as a technique of analyzing variability;
- appropriate visualization of the results.

The experimental results show the interest of the proposed approach for variability analysis and data reduction. In the illustrated example for the left lateral ventricle, we could express the major contribution of variability with only three components.

Further work aims at analyzing in more detail the influence of the parameters of the method, and comparing the results with those obtained using independent component analysis (Cardoso and Comon, 1996). Experiments on other brain structures will be carried out as well. A potential application could be to compare the observed variations in different populations (normal and pathological ones for instance).

ACKNOWLEDGEMENTS

This work has been partly supported by an ECOS-Nord grant, Darwin Martinez is supported by a COLCIENCIAS-Bonpland grant and Universidad de los Andes project CIFI-56 of 2008.

REFERENCES

- Bai, B., Kantor, P., Shokoufandeh, A., and Silver, D. (2007). fMRI brain image retrieval on ICA components. In *Proceedings of ENC'07*, pages 10–17.
- Berar, M. (2007). *Modèles statistiques de la forme d'organes du corps humain, application à la reconstruction faciale*. PhD thesis, Institut National Polytechnique de Grenoble, Grenoble, France.
- Besl, P. J. and McKay, N. D. (1992). A method for registration of 3-d shapes. *IEEE Transactions on Pattern Analysis and Machine Intelligence*, 14(2):239–256.
- Borgefors, G. (1986). Distance transformations in digital images. *Computer Vision, Graphics, and Image Processing*, 34(3):344–371.
- Cardoso, J.-F. and Comon, P. (1996). Independent component analysis, a survey of some algebraic methods. In *ISCAS'96: 1996 IEEE International Symposium on Circuits and Systems*, volume 2, pages 93–96.
- Cootes, T. F., Edwards, G., and Taylor, C. J. (2001). Active appearance models. *IEEE Transactions on Pattern Analysis and Machine Intelligence*, 23(6):681–685.
- Ekenel, H. K. and Sankur, B. (2004). Feature selection in the independent component subspace for face recognition. *Pattern Recognition Letters*, 25(12):1377–1388.
- Hill, A., Cootes, T. F., and Taylor, C. J. (1996). Active shape models and the shape approximation problem. *Image and Vision Computing*, 14(8):601–607.
- Larsen, R. and Hilger, K. B. (2003). Statistical shape analysis using non-Euclidean metrics. *Medical Image Analysis*, 7(4):417–423.
- Lötjönen, J., Kivistöb, S., Koikkalainen, J., Smuteka, D., and Lauerma, K. (2004). Statistical shape model of atria, ventricles and epicardium from short- and long-axis MR images. *Medical Image Analysis*, 8:371–386.
- Moreno, A., Chambon, S., Santhanam, A., Rolland, J., Angelini, E., and Bloch, I. (2007). CT-PET Landmark-based Registration using a Dynamic Lung Model. In *International Conference on Image Analysis and Processing ICIAP 2007*, pages 691–696, Modena, Italy.
- Moreno, A., Chambon, S., Santhanam, A., Rolland, J., Angelini, E., and Bloch, I. (2008). Combining a Breathing Model and Tumor-Specific Rigidity Constraints for Registration of CT-TEP Thoracic Data. *Computer Aided Surgery*, 13(5):281–298.
- Nain, D., Haker, S., Bobick, A., and Tannenbaum, A. (2007). Multiscale 3-D shape representation and segmentation using spherical wavelets. *IEEE Transactions on Medical Imaging*, 26(4):598–618.
- Pohl, K. M., Warfield, S. K., Kikinis, R., Grimson, W. E. L., and Wells, W. M. (2004). Coupling statistical segmentation and PCA shape modeling. In *Medical Image Computing and Computer-Assisted Intervention MICCAI 2004*, volume LNCS 3216, pages 151–159.
- Rogez, G. and Orrite, C. (2005). Human figure segmentation using independent component analysis. In *IbPRIA Pattern Recognition and Image Analysis*, volume LNCS 3522, pages 300–307.
- Suinesiaputra, A., Üzümcü, M., Frangi, A., Kaandorp, T., Reiber, J., and Lelieveldt, B. (2004). Detecting regional abnormal cardiac contraction in short-axis MR images using independent component analysis. In *Medical Image Computing and Computer-Assisted Intervention*, volume LNCS 5032, pages 737–744.
- Taron, M., Paragios, N., and Jolly, M.-P. (2007). From uncertainties to statistical model building and segmentation of the left ventricle. *ICCV 2007. IEEE 11th International Conference on Computer Vision*, pages 1–8.
- Yang, Q. and Ding, X. (2002). Symmetrical PCA in face recognition. In *International Conference on Image Processing*, volume 2, pages 97–100.